



Encapsulating Anti-Parasite Benzimidazole Drugs into Lipid-Coated Calcium Phosphate Nanoparticles to Efficiently Induce Skin Cancer Cell Apoptosis

Fatemeh Movahedi¹, Wenyi Gu¹, Christiane Pienna Soares² and Zhi Ping Xu^{1*}

¹Australian Institute for Bioengineering and Nanotechnology (AIBN), The University of Queensland, St Lucia, QLD, Australia, ²Department of Clinical Analysis, School of Pharmaceutical Sciences, Universidade Estadual Paulista (UNESP), Araraquara, Brazil

OPEN ACCESS

Edited by:

Zhiqing Pang,
Fudan University, China

Reviewed by:

Bo Zhang,
Huazhong University of Science and
Technology, China
Wei He,
China Pharmaceutical University,
China
Raj Kumar,
University of Michigan, United States

*Correspondence:

Zhi Ping Xu
gordonxu@uq.edu.au

Specialty section:

This article was submitted to
Biomedical Nanotechnology,
a section of the journal
Frontiers in Nanotechnology

Received: 12 April 2021

Accepted: 28 May 2021

Published: 15 June 2021

Citation:

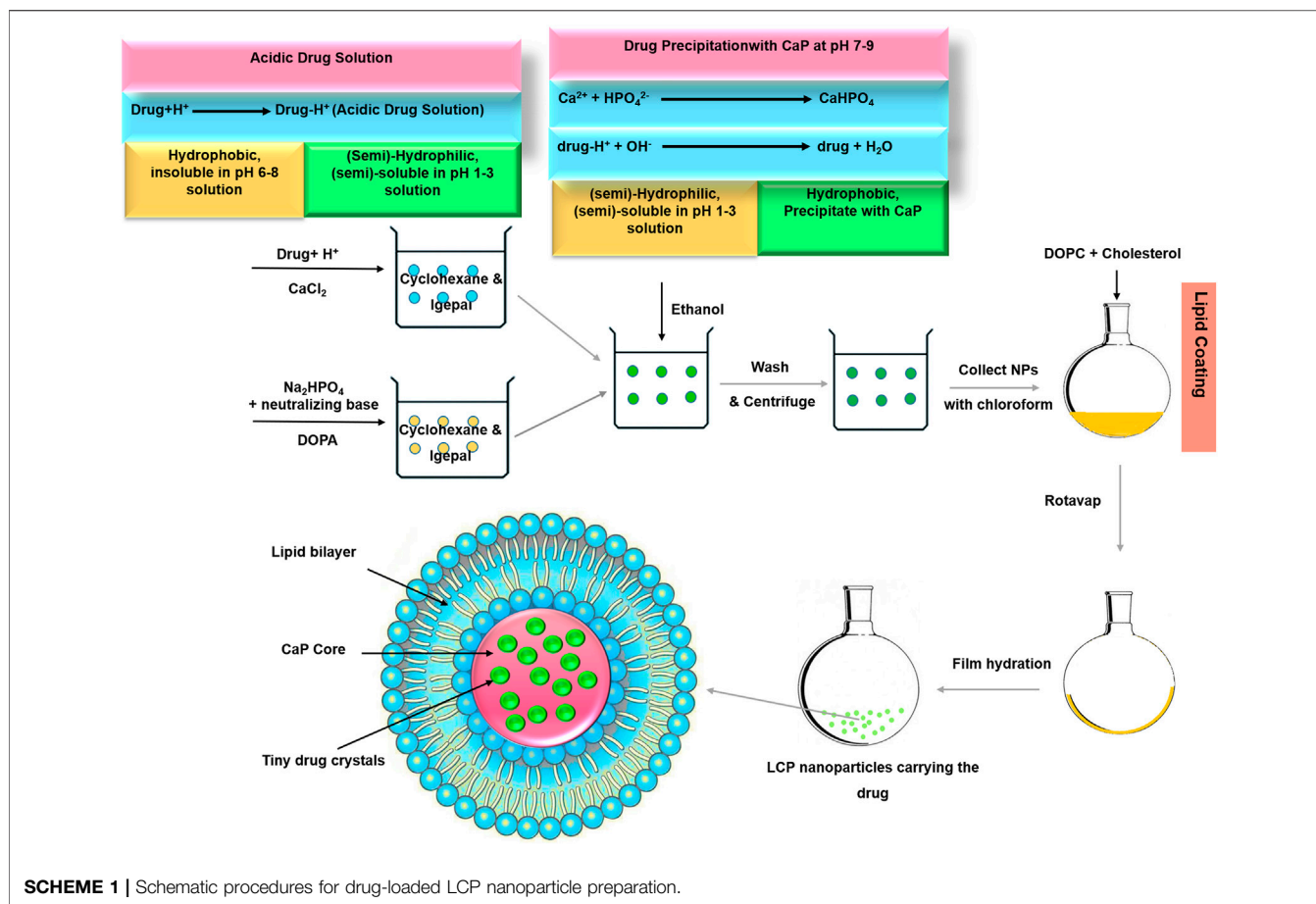
Movahedi F, Gu W, Soares CP and
Xu ZP (2021) Encapsulating Anti-
Parasite Benzimidazole Drugs into
Lipid-Coated Calcium Phosphate
Nanoparticles to Efficiently Induce Skin
Cancer Cell Apoptosis.
Front. Nanotechnol. 3:693837.
doi: 10.3389/fnano.2021.693837

Benzimidazole (BMZ) family of anti-worm drugs has been now repurposed as anti-cancer drugs. However, offering a general reformulation method for these drugs is essential due to their hydrophobicity and low aqueous solubility. In this work, we developed a general approach to load typical BMZ drugs as tiny nanocrystals within lipid-coated calcium phosphate (LCP) nanoparticles. BMZ drug-loaded LCP nanoparticles increased their solubility in PBS by 100–200% and significantly enhanced the anti-cancer efficacy in the treatment of B16F0 melanoma cells. These drug-LCP nanoparticles induced much more cancer cell apoptosis, generated much more reactive oxygen species (ROS) and inhibited Bcl-2 expression of cancer cells. Moreover, BMZ drug-loaded LCP nanoparticles caused morphological change and extension disruption of cancer cells, and significantly reduced migration activity, representing high possibility for inhibition of tumor dissemination and metastasis. Very advantageously, BMZ drug-loaded LCP nanoparticles did not show any obvious toxicity, Bcl-2 inhibition and morphological changes in HEK293T healthy cells. In conclusion, BMZ drug-incorporated LCP nanoformulations may be a valuable nanomedicine that is able to inhibit primary tumors and prevent tumor dissemination with minimum side effects on healthy cells and tissues.

Keywords: benzimidazole family of anti-worm drugs, lipid-coated calcium phosphate nanoparticles, enhanced solubility, enhanced anti-cancer toxicity, inhibition of cancer dissemination

INTRODUCTION

Benzimidazoles (BMZs) are a family of anti-helminth drugs widely used in humans and livestock since 1960s to treat parasitic infections (Stasiuk et al., 2019). Many members of this family including albendazole (ABZ), fenbendazole (FBZ), mebendazole (MBZ) and thiabendazole (TBZ), are cost-effective FDA-approved drugs which are associated with very mild side effects (Carvalho and Gadelha, 2007). In recent years, many studies have reported the anti-cancer effect of these drugs on a broad range of cancers (Noorani et al., 2015; Castro et al., 2016). The new findings have a great importance not only because of offering cancer chemotherapeutics with minimum side effects but also due to the considerable reduction of Research and Development (R & D) and commercialising



costs compared to the costs of developing new anti-cancer agents, a substantial challenge of global pharmaceutical industry at the moment (Pushpakom et al., 2018).

Because of various similarities between parasites and cancer cells (Dorosti et al., 2014), benzimidazole drugs are also potent to suppress cancer through anti-parasite mechanisms such as inhibiting tubulin polymerization, disrupting the formation of mitotic spindle, causing cell cycle arrest, and inducing apoptosis (Hasanpourghadi et al., 2016). However, the clinical anti-cancer application of these drugs is still limited due to low aqueous solubility and limited bioavailability (Daniel-Mwambete et al., 2004).

Providing a small size and a large surface area to volume ratio, nanoformulation has been considered as a promising approach for repositioning the poorly water-soluble drugs such as BMZs (Kumar et al., 2020) by improving their solubility, dissolution rate and bioavailability (Thorat and Dalvi, 2012). In addition, nanoparticles provide the possibility of drug penetration through the tight junctions of the skin and blood brain barrier as well as offering enhanced permeability and retention (EPR) effect, stimuli-responsive and targeted delivery (Kohane, 2007). Having the benefits of both calcium phosphate (CaP) nanoparticles and liposomes, lipid-coated calcium phosphate (LCP) nanoparticles are considered as ideal carriers for nanoformulation of BMZ drugs due to pH-responsiveness,

controlled size and the possibility for targeted delivery (Tang et al., 2015).

To demonstrate the capability of LCPs as benzimidazole drug carriers for the general cancer therapy, it is essential to examine apoptosis induction in tumor cells, inhibit resistance-mediating factors such as B-cell lymphoma 2 (Bcl-2), and reduce tumor cell dissemination. As schematically shown in Scheme 1, our new approach for preparing ABZ-loaded lipid-coated calcium phosphate (LCP) nanoparticles (Movahedi et al., 2020) is generalized. Since BMZ-drug is protonated and dissolved in acidic aqueous solution, BMZ drug is first dissolved in acidic CaCl_2 solution, which is then made into the first W/O emulsion. The second W/O emulsion is made to contain phosphate and base, which will neutralize and precipitate upon mixing with the first emulsion. During the mixing, protonated BMZ-drug molecules are neutralized and then precipitate as tiny nanocrystals within the simultaneously precipitated calcium phosphate matrices, which are then encapsulated with the lipid bilayer after hydration (Scheme 1). Such LCP nanoparticles are expected to retain the tiny drug crystals within CaP nanoparticles in physiological solution but release the drug in a pH-responsive way upon exposure to acidic organelles (endosome and lysosome) in tumor cells, leading to enhanced anti-cancer efficacy due to facilitated cellular uptake and improved solubility.

The objectives of this research were thus to: 1) generalize our approach for preparation of BMZ drug-loaded LCP nanoparticles (such as ABZ, FBZ, MBZ, and TBZ); 2) show enhanced solubility of these drugs in the LCP nanoparticle form; 3) confirm the cytotoxic effect against B16F0 melanoma cells but not healthy cell line HEK293T in the LCP form; and 4) demonstrate the apoptosis-induced mechanisms, such as inhibition of Bcl-2 expression and overproduction of reactive oxygen species (ROS), morphological changes and reduction of tumor cell migration. This research has specifically shown the potential of BMZ-LCP nanoparticle formulations as promising anti-cancer nanomedicines.

MATERIALS AND METHODS

Materials

Albendazole (ABZ), fenbendazole (FBZ), mebendazole (MBZ), thiabendazole (TBZ), igepal-CO520, calcium chloride, sodium phosphate, DMSO and cholesterol were purchased from Sigma-Aldrich, cyclohexane from Merck (Germany), and 1,2-dioleoyl-sn-glycero-3-phosphate (DOPA) and 1,2-dioleoyl-sn-glycero-3-phosphocholine (DOPC) from Avanti polar lipids. MTT [3-(4,5-Dimethylthiazol-2-yl)-2,5-diphenyltetrazolium bromide] was obtained from Invitrogen and 2',7'-dichlorodihydrofluorescein diacetate (H2DCFDA) from Promokine (Germany). Apoptosis kit was provided by Biolegend and Bcl-2 FITC Antibody was purchased from eBioscience. All other chemicals were obtained from Sigma-Aldrich unless indicated. Water was deionised Milli-Q water (18.2 M Ω cm at ambient temperature).

Lipid-Coated Calcium Phosphate Nanoparticle Preparation and Characterisation

In order to synthesise drug-loaded LCPs (ABZ/FBZ/MBZ/TBZ-LCP), drugs were incorporated into calcium phosphate core of LCPs as illustrated in Scheme 1. In brief, acidic drug solution (625–5,000 μ g/ml) in CaCl₂ aqueous solution was dispersed in cyclohexane/Igepal CO-520 (7/3 v/v) to prepare a well-dispersed microemulsion. After stirring for 10 min, the microemulsion was mixed with the other well-dispersed DOPA (20 mM in chloroform)-containing W/O microemulsion consisting of aqueous solution of ammonia and Na₂HPO₄. After stirring for another 20 min, absolute ethanol was added to collect drug-loaded calcium phosphate (CaP) cores by centrifugation at 10,000 g for 20 min and washing with absolute ethanol thrice. CaP cores were then redispersed in chloroform and mixed with cholesterol and DOPC chloroform. Chloroform was evaporated under reduced pressure and the resultant film was hydrated with PBS (pH 7.4), followed by gentle ultrasonication to obtain the well dispersed LCP NP suspension.

As summarized in **Supplementary Table S1** ABZ/FBZ/MBZ/TBZ-LCP #1-4 were denoted for nanoparticles prepared at various drug concentrations in acidic solutions (630, 1,250, 2,500 and 5,000 μ g/ml), respectively.

The hydrodynamic diameter, PDI and zeta potential of drug-loaded LCPs were determined by Zetasizer (DLS, Zetasizer Nano, Malvern, United Kingdom). The microscopic images of drug-loaded LCP NPs were taken in a transmission electron microscope (TEM, JEM-3010, ZEOL, Tokyo, Japan) operated at the voltage of 100 kV.

To determine the encapsulation efficiency, drug-loaded LCP NPs were incubated with Tris Buffer (2 mM EDTA and 0.05% Triton X-100 in pH 7.8) at 65°C for 10 min. The resultant samples were centrifuged for 15 min at 20,000 g, and the drug concentration in the supernatant was calculated by the absorbance measured at 290 nm for albendazole (ABZ), 305 nm for fenbendazole (FBZ), 235 nm for mebendazole (MBZ) and 300 nm for thiabendazole (TBZ), respectively.

Cell Growth Inhibition

The growth inhibition of B16F0 cells and HEK293T cells by BMZ family drugs in the free form and the LCP form was assessed by MTT assay. Briefly, 4,000 cells in 100 μ l of DMEM per well were seeded in a 96-well plate after incubation overnight at 37°C and 5% CO₂. Then, culture medium was replaced with fresh one containing variable amounts of drugs in the free or LCP form (ABZ/FBZ/MBZ/TBZ-LCP) and cells were incubated for 24 h. After removal of culture medium, MTT in DMEM (5 mg/ml) was added and incubated for another 4 h at 37°C and 5% CO₂. Then, DMEM containing MTT was carefully removed and replaced with 50 μ l DMSO to dissolve formazan crystals. After shaking the plate for 10 min, the absorbance was read at 570 nm, and cell viability was calculated based on the absorbance compared to that of untreated cells.

Apoptosis Analysis

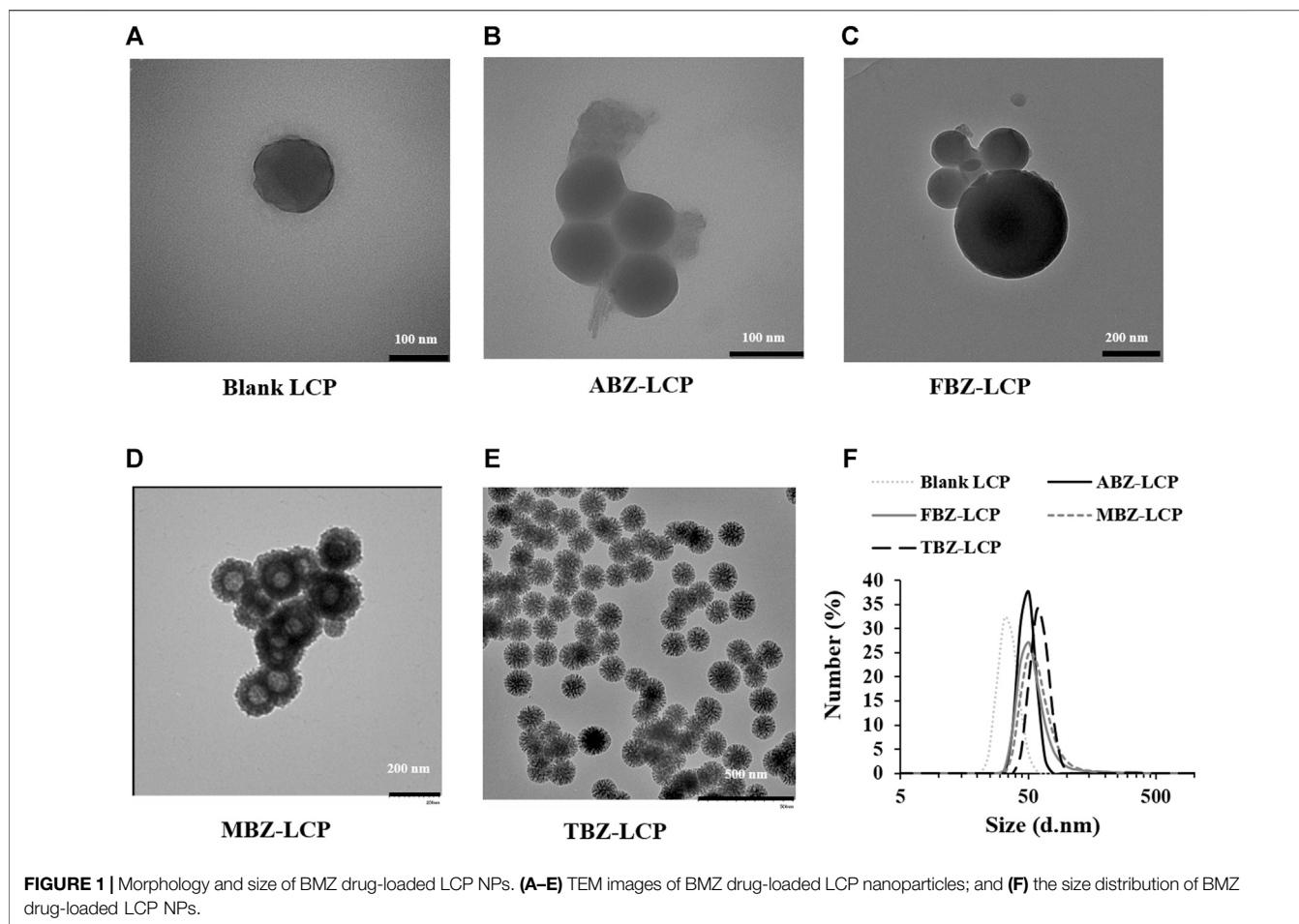
B16F0 cells were treated with BMZ drugs in the free or LCP form for 24 h. The cells were then detached by trypsinisation (0.25% trypsin) and centrifuged at 2000 rpm for 5 min. Resultant cell pellets were washed with PBS and resuspended in 100 μ l of Annexin V Binding Buffer and added with 5 μ l of FITC Annexin V and 10 μ l of propidium iodide solution. After incubation for 15 min in dark, 400 μ l of Annexin V Binding Buffer was added to each tube and fluorescence of the cells was evaluated with a flow cytometer (CytoFLEX, Beckman, United States) and analysed by CytExpert software.

Reactive Oxygen Species Detection

B16F0 or HEK293T cells were treated with BMZ drugs in the free or LCP form for 6 h at 37°C and 5% CO₂, and then co-cultured with 2',7'-dichlorodihydrofluorescein diacetate (20 μ M) for 30 min. The cells were collected and analysed in a flow cytometer (CytoFLEX, Beckman, United States).

Bcl-2 Detection

To determine the level of Bcl-2, cells were incubated in DMEM media with drug-loaded LCP NPs for 24 h at 37°C and 5% CO₂, then detached by trypsinisation (0.25% trypsin) and centrifuged at 2000 rpm for 5 min, followed by washing with PBS twice. Then, cold fixation buffer (2% PFA) was added dropwise while vortexing the cells. After incubating for at least 30 min at 4°C, cells were



centrifuged for 5 min at 300 g and washed twice with cold PBS. Cells were then resuspended in permeabilisation buffer (0.1% in triton-X in PBS) and incubated for 15 min at room temperature, followed by centrifugation for 5 min and washing twice with PBS. Afterward, 150 μ l of blocking buffer (0.5% BSA, 2% FBS in PBS) was added to cells. The cells were vortexed and incubated for 30 min, then centrifuged and resuspended in 100 μ l of antibody solution, followed by incubation for another 30 min on ice in dark. Samples were washed twice with FACS buffer (2% FBS in PBS) and analysed using a flow cytometer (CytoFLEX, Beckman, United States) or spectrophotometer.

Migration Assay

To evaluate the effect of the treatment on migration activity of B16F0 or HEK293T cell line, cells were incubated in a 12-well plate overnight to form a confluent monolayer. Then the scratch was artificially made using a 100 μ l pipette tip. The suspended cells and debris were washed away with PBS twice, and the cells in the plate were incubated in DMEM containing free drugs or drug-loaded LCP NPs for 4 h. Olympus IX81 microscope was used to take the images and the relative migration was calculated as the percentage of the number of control cells.

Statistical Analysis

Data presented as mean \pm SD were analysed by t-test using GraphPad 7.03 software. The p value less than 0.05 was considered as statistically significant. $p < 0.05$: *; $p < 0.01$: **; $p < 0.001$: ***.

RESULTS AND DISCUSSION

General Physicochemical Characteristics of Benzimidazole Family-Loaded Lipid-Coated Calcium Phosphate Nanoparticles

As demonstrated in TEM images (Figure 1), all typical LCP NPs, i.e., loaded with about 15 wt% of drug molecules, were spherical in shape. The average size and the size distribution of these typical drug-loaded LCP NPs were very similar (Figure 1E; Table 1) with a similar distribution profile (polydispersity index (PDI) of 0.3–0.4). Relatively, FBZ-LCP and ABZ-LCP NPs were smaller with the number-mean diameter of 44.0 ± 5.1 and 49.5 ± 6.3 nm, respectively, while MBZ-LCP and TBZ-LCP NPs had the number-mean diameter of 58.8 ± 5.3 and 57.8 ± 4.2 nm

TABLE 1 | The average size, PDI and the zeta potential of typical LCP NPs loaded with about 15 wt% of BMZ drugs.

Sample	Size (d.nm)	PDI	Zeta Potential (mV)	Encapsulation Efficiency (%)	Loading Capacity (wt%)
Blank LCP	35.7 ± 5.2	0.32 ± 0.06	-17.0 ± 3.1	-	-
ABZ-LCP	49.5 ± 6.3	0.35 ± 0.10	-16.5 ± 4.9	65.4	14.9
FBZ-LCP	44.0 ± 5.1	0.36 ± 0.08	-17.1 ± 2.5	80.0	15.6
MBZ-LCP	58.8 ± 5.3	0.33 ± 0.05	-19.1 ± 4.8	40.0	15.6
TBZ-LCP	57.8 ± 4.2	0.39 ± 0.03	-16.4 ± 4.7	39.1	15.3

(Table 1). In specific, MBZ-LCP NPs had a clear core with the diameter of ~40 nm and a thick layer (~30 nm) as well as a very rough surface (Figure 1D). The core size seems to be very similar to that of ABZ-LCP and FBZ-LCP NPs (Figures 1B,C). In contrast, the cores were not seen in TBZ-LCP NPs, which had a very hairy surface (Figure 1E). While factors such as calcium/phosphate molar ratio and mixing style affect the size of LCPs, the optimized condition was adopted from previous studies in our lab (Tang et al., 2015) to achieve the mean size of LCPs lying in the ideal range for cancer therapy to avoid recognition by the immune system (>200 nm) or clearance by kidneys (<5 nm) (Liu et al., 2013).

The surface charge of all drug-loaded LCP NPs was almost similar, varying from -19 to -16 mV. The negative surface charge of LCPs would reduce the adsorption of serum proteins, and benefit the prolonged half-life in blood circulation and enhanced tumor accumulation of NPs (Blanco et al., 2015).

Variable Loading and Enhanced Solubility of Benzimidazole Drugs in Lipid-Coated Calcium Phosphate NPs

Alteration in encapsulation efficiency and loading capacity was examined by varying the initial concentration of BMZ family drugs in the nanoemulsion, as illustrated in Figure 2; Supplementary Table S1. The loading capacity of these drugs was varied from 0–15.3% (TBZ) to 0–23.2% (FBZ) (Supplementary Table S1). In general, the encapsulation efficiency (EE) was relatively high (>50%). Especially, the EE was 60–85% and 59–93% for ABZ and FBZ, and 40–80% and 39–67% for MBZ and TBZ, respectively. The lower encapsulation efficiency for MBZ and TBZ may stem from their relatively higher aqueous solubility of these two drugs in PBS, particularly in the case with the high drug loading (Supplementary Table S1).

As represented in Figure 3, the commercial MBZ and TBZ were found to have a solubility of 30 and 45 µg/ml, while it was 10 and 6 µg/ml for commercial ABZ and FBZ, respectively, which are similar to that reported for these anti-parasite drugs elsewhere. For example, the solubility of TBZ was reported to be 50 µg/ml at 25°C (Thiabendazole-DrugBank), MBZ 1–70 µg/ml in physiological conditions (Swanepoel et al., 2003) and that of ABZ and FBZ 1–8 µg/ml (at pH 6–8) (Kang et al., 2015) and 6 µg/ml in physiological conditions (Ryu et al., 2013), respectively. Consequently, the higher aqueous solubility of MBZ and TBZ may lead to a lower precipitation rate during formation of CaP

cores, resulting in a smaller amount of the drug being encapsulated.

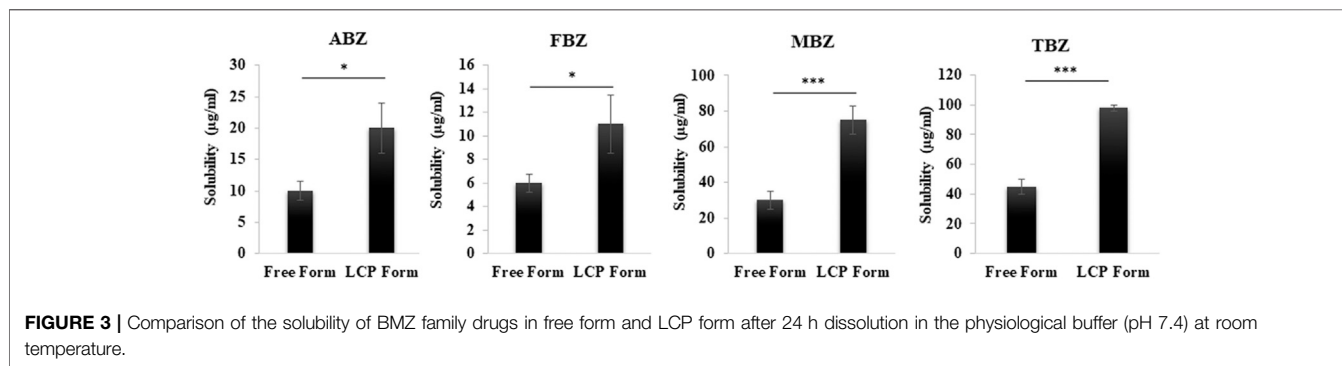
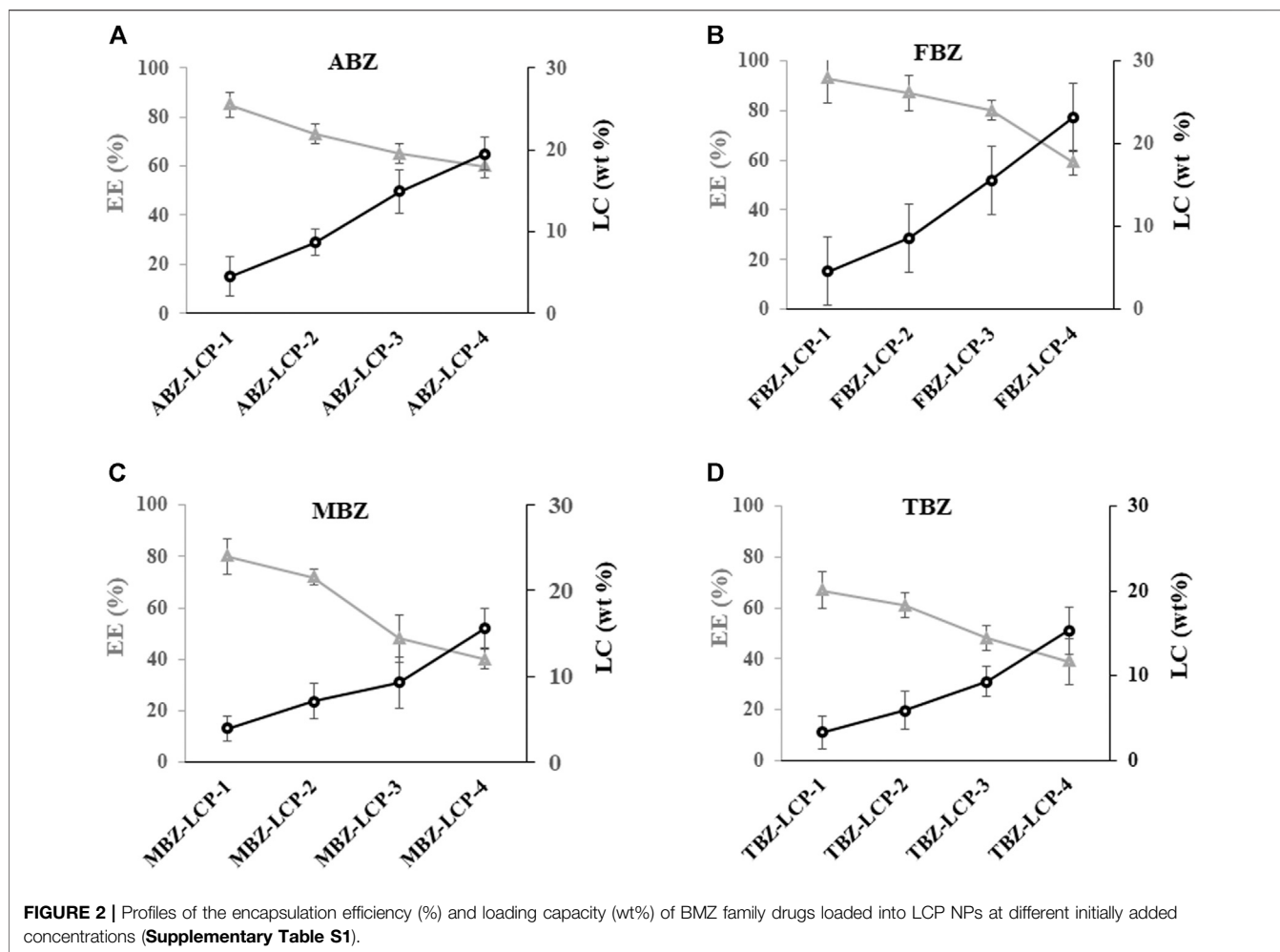
Furthermore, as demonstrated in Figure 3; Supplementary Table S2, the solubility of all drugs was almost doubled in the LCP form. As discussed in our previous study, the enhanced solubility arises from incorporation of tiny drug nanocrystals in the CaP matrix (a few nm in size) -with crystalline structure confirmed by XRD results-, which is significantly smaller than very large crystals in the free form of commercial drugs (>1,000 nm confirmed by TEM imaging) (Movahedi et al., 2020). After the lipid bilayer and the CaP matrix are dissolved partly (particularly in acidic environment of tumor), the tiny drug nanocrystals are exposed to the aqueous phase and dissolved much more than large crystals (commercial products) due to enhanced surface area, thinner diffusion layer and higher differential concentration (Kumar et al., 2020). Melian et al., also have reported the improved solubility of fenbendazole by nanocrystallisation (Melian et al., 2020). Additionally, at lower pH of tumor environment, the released drug becomes more hydrophilic due to protonation process of the aromatic amines (Chen et al., 2015).

We further hypothesise that some surface MBZ and TBZ tiny nanocrystals may be already dissolved partially during hydration, and the left LCP-BMZ cores may interact the lipid molecules and form some complex structures, such as a hairy/rough surface, as observed in TEM images (Figures 1D,E).

In summary, LCP-based BMZ drug-loaded NPs were controllably made in the number-mean diameter of 40–60 nm with the BMZ drug loading capacity varying from 0 to ~25 wt%. Once encapsulated in LCP NPs, these hydrophobic BMZ drugs showed a double solubility in PBS. Thus the preparation approach would be a general strategy for encapsulating acid-soluble hydrophobic drugs into the CaP matrix, a general way to enhance the bioavailability and activity of the drugs, as presented in the following sections, taking these MBZ-loaded LCP NPs as examples for the cellular anti-cancer therapy.

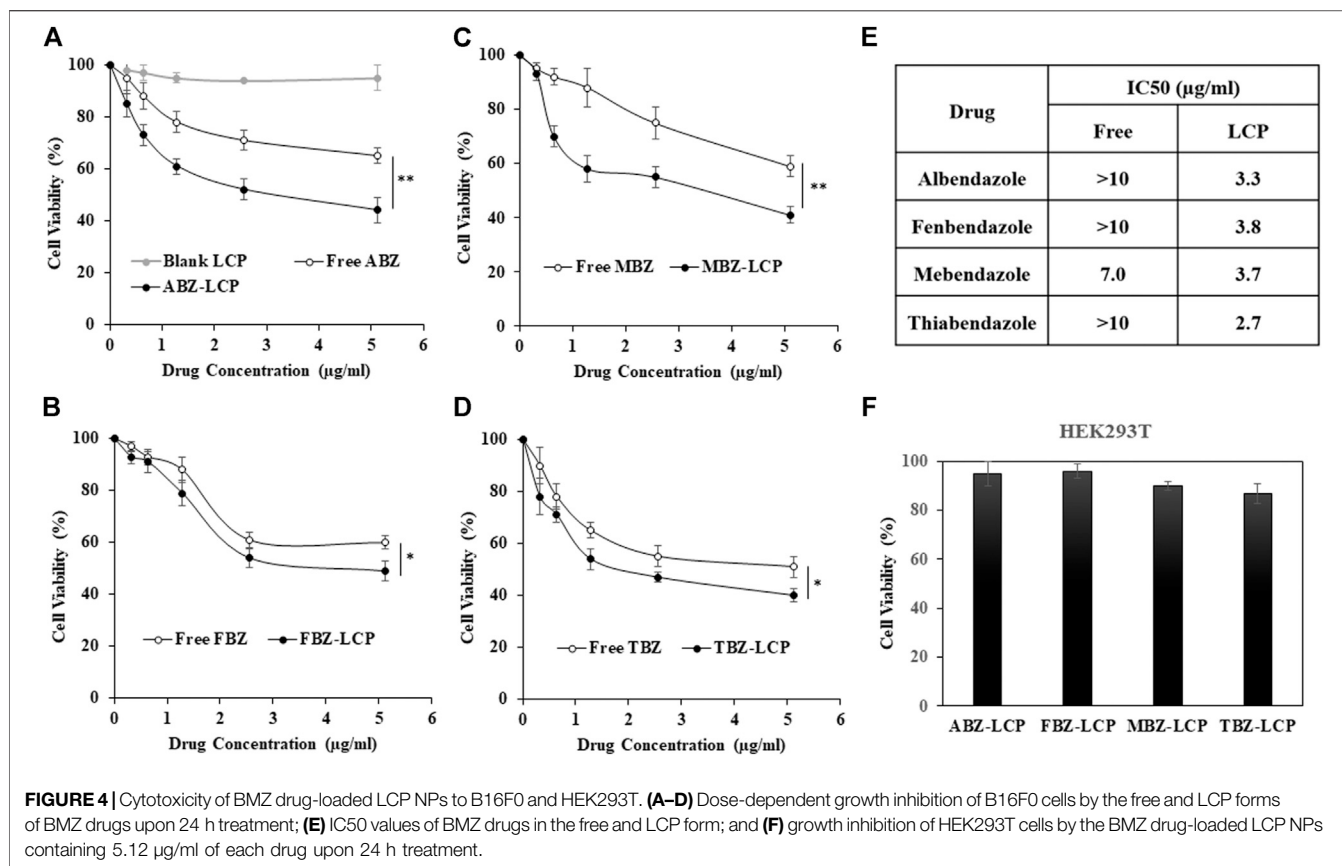
In Vitro Cell Growth Inhibition by Benzimidazole-Loaded Lipid-Coated Calcium Phosphates

The cytotoxic effect of BMZ family drugs in the free and LCP forms is shown in Figure 4. No B16F0 toxicity was observed for blank LCP NPs (Figure 4A). All drugs demonstrated a dose-dependent anti-cancer effect against B16F0 cells in both forms, while BMZ-LCP NPs were significantly more active



than that of their corresponding free form (Figures 4A–D). Approximately, IC₅₀ values (Figure 4E) were varied from 7 to >10 µg/ml for the free drugs. In sharp contrast, the IC₅₀ value was remarkably decreased to 2.7–3.8 µg/ml for their corresponding LCP forms. Enhanced cytotoxicity of BMZ-LCP NPs may come from improved solubility, as discussed previously, and moreover, facilitated cellular uptake via LCP NP carriers (Wu et al., 2017).

The reported anti-cancer effect of these BMZ drugs in their free form is comparable to our observations. For example, 85% cell viability was observed after 24 h treatment of B16F0 melanoma cells at 0.32 µg/ml of free ABZ, which is very similar to 90% cell viability for A375 and A2058 melanoma cell lines after 12 h treatment at 1 µM (0.265 µg/ml) of ABZ and ~70% after 72 h treatment (Patel et al., 2011). B16F0 cell viability was 54 and 49% at 2.56 and 5.12 µg/ml of free FBZ in the



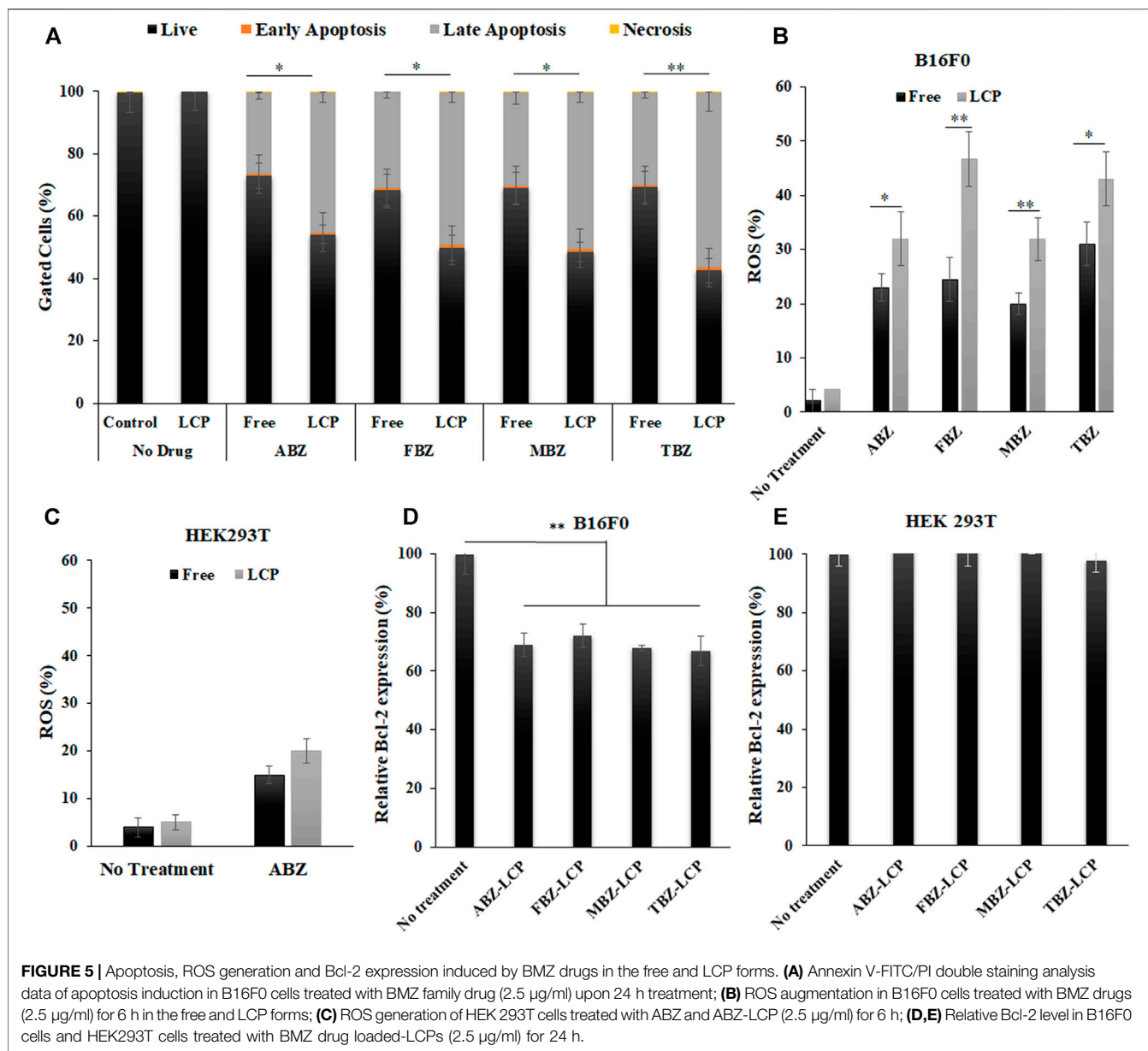
current test, which is similar to 40% viability of EMT6 cells upon treatment with 10 μM (4 $\mu\text{g/ml}$) of FBZ (Duan et al., 2013). Similarly, MBZ showed some anti-cancer effect on cell lines such as MCF7, T47D, and MDA-MB-231 breast cancer (Zhang et al., 2019) in the drug dosage range of 1–10 μM (0.3–3 $\mu\text{g/ml}$). In addition, daily intraperitoneal injections of 50 mg/ml TBZ led to almost 75% tumor reduction in the HT1080 fibrosarcoma xenograft mouse model after 27 days treatment, representing high anti-cancer efficacy of this drug (Cha et al., 2012). Clearly, LCP-based BMZ drug NPs developed in this research have demonstrated much higher anti-cancer activity than their free forms, which is the motivation of this research to repurpose these anti-parasite drugs for anti-cancer therapy.

Very interestingly, the highest drug dosage examined in the LCP form showed no obvious toxicity to healthy cell line HEK293T (Figure 4F). This is similar to that no obvious toxicity to HUVEC healthy cells was observed after treatment with MBZ at the dosage highly toxic to lung cancer cell lines (Mukhopadhyay et al., 2002). Similarly, ABZ did not show any toxicity to HOSE normal ovary cells, but to ovarian cancer cell lines in the similar dose range (Noorani et al., 2015). Thus, the safety of BMZ family drugs is a principal advantage over many chemotherapeutics as these drugs have the minimum side effects on healthy tissues/organs and are widely used orally by humans at the dose of up to 15–20 mg/kg every day for an adult (Despommier et al., 2017).

Apoptosis Induction through Reactive Oxygen Species Augmentation and Bcl-2 Inhibition

Apoptosis induction by BMZ family drugs in the free form and the LCP form was analyzed by Annexin V-FITC/PI double staining method (Supplementary Figure S1). As represented in Figure 5A, both forms of drugs induced major late apoptosis while the LCP form induced a much higher level of late apoptosis (45–56% compared to 26–30% for the free drugs). There was also a few percent of early apoptosis and necrosis in all treatments. The elevated later apoptosis may be the reason behind the higher cytotoxic effect of these drugs in the LCP form, which may be attributed to the enhanced solubility and facilitated cellular uptake of drugs via the LCP NP carriers (Tang et al., 2015).

Since the defect in apoptosis plays a fundamental role in cancer pathogenesis, providing time for genetic mutation, increasing angiogenesis and promoting invasion apoptosis induction is considered as the most promising non-surgical approach for cancer therapy (Pfeffer and Singh, 2018). Some studies have confirmed apoptosis induction in cancerous cells by BMZ family drugs. These reported data included 30% apoptosis of human NSCLC cells induced with 1 μM (0.3 $\mu\text{g/ml}$) of FBZ for 32 h and 50% of Ehrlich carcinoma cells in animals with 20 mg/kg of ABZ (Castro et al., 2016).



Both the free and LCP forms of BMZ drugs elevated the ROS level in B16F0 cells, as demonstrated in **Figure 5B**; **Supplementary Figure S2**. Similar to apoptosis induction, the ROS level was augmented much higher upon treatment with the LCP form of BMZ drugs (32–47%) than that with the free form of drugs (20–31%). As reported by Castro et al., ROS in MCF7 cells was overgenerated upon treatment with 25 µM (6.6 µg/ml) of ABZ for 1 h (Castro et al., 2016), and treating A549 cells with 10 µM (3 µg/ml) of FBZ for 4 h significantly enhanced ROS production (Dogra and Mukhopadhyay, 2012). Since ROS plays a key role in regulation of cell signalling and pathways of apoptosis, ROS augmentation may be responsible for enhanced apoptosis in drug-loaded LCP NP-treated cells.

ROS enhancement was much lower in the healthy cells, e.g., HEK293T cells treated with both free ABZ and ABZ-LCP NPs

(**Figure 5C**; **Supplementary Figure S3**). Considerably lower ROS induction by ABZ -as the representative of BMZ drugs- in HEK293T cells was demonstrated just to support the fact that these drugs are selectively toxic on cancer cells by unbalancing the ROS level. In comparison with cells treated without any drugs, ROS enhancement was 10–20 fold in drug-treated B16F0 cells (**Supplementary Figure S2**), but it was only 1.5–2.5 fold in drug-treated HEK293T (**Supplementary Figure S3**). This may be the reason that increased ROS generation by only 1.5–2.5 fold did not affect HEK293T cell viability (**Figure 4F**). Thus ROS generation enhanced by BMZ-LCP NPs can selectively kill cancer cells but not healthy cells, as a selective approach for cancer therapy (Perillo et al., 2020).

Consistently, the relative level of Bcl-2 (**Figure 5D**) was all significantly dropped in B16F0 cells after treatment with

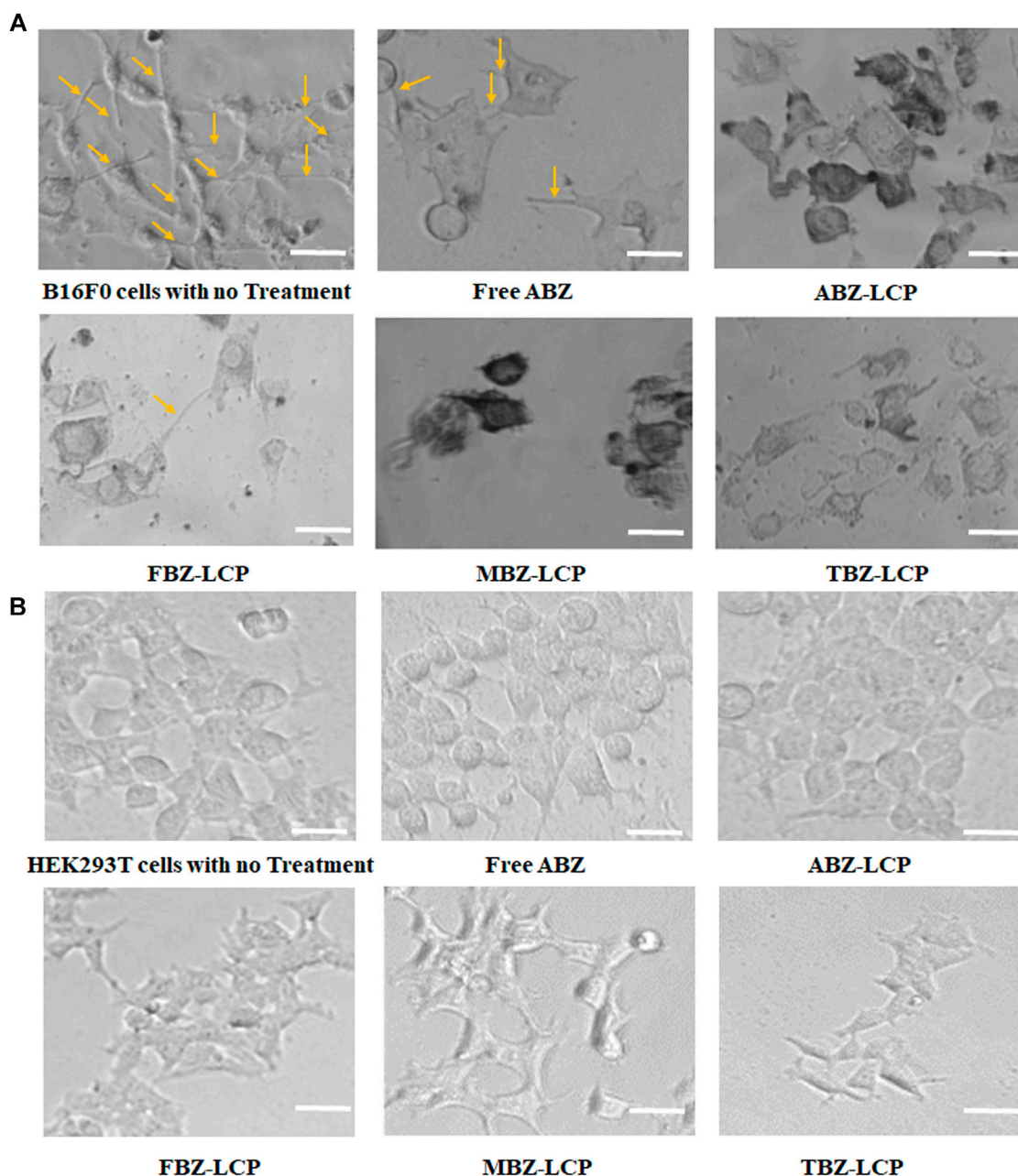
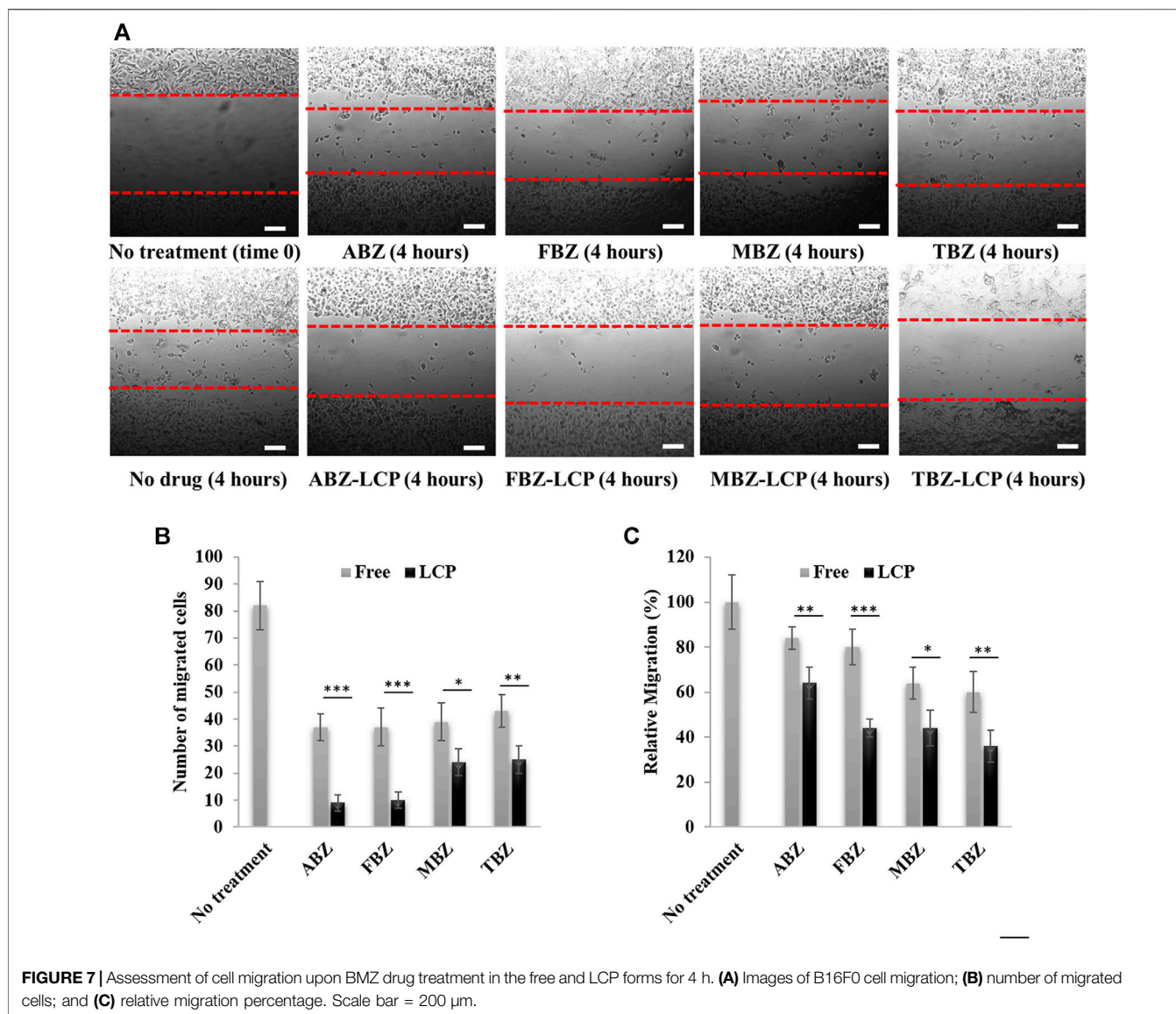


FIGURE 6 | Effect on cell morphology. **(A)** Morphology changes of B16F0 cells treated with BMZ drug-loaded LCP NPs (2.5 µg/ml); and **(B)** The similar morphology of HEK293T cells upon ABZ treatment at 2.5 µg/ml in the free and LCP forms. Scale bar = 50 µm.

drug-loaded LCP NPs, with 28–34% reduction compared to untreated cells. Since cancer cells normally overexpress Bcl-2, the pro-survival founder member of Bcl family (Campbell and Tait, 2018), and protect themselves from ROS-mediated apoptosis induction through the activation of endogenous antioxidants (Hildeman et al., 2003), Bcl-2 inhibition by BMZ drug-loaded LCP NPs further contributes to inducing apoptotic response in addition to ROS overproduction. This observation is consistent with the report that ABZ reduced the expression of apoptosis-related

proteins such as Bcl-2, Bcl-xL, Bax and Bad (Doudican et al., 2008).

Once again, no obvious alteration in the Bcl-2 level was observed in HEK293T cells (Figure 5E) upon the same treatment with BMZ drug-loaded LCP NPs, indicating the safety of the drugs to healthy cells. This is also similar to the report that melanocytes did not alter the Bcl-2 expression even after MBZ treatment (Doudican et al., 2008). Thus the comparison between B16F0 cancer cells and HEK293T healthy cells may reveal that BMZ drug treatment in free or LCP form just



inhibits the overexpressed Bcl-2 in cancer cells but does not interfere the general Bcl-2 level in the normal cell line.

Morphological Changes and Cell Migration Inhibition

Treatment of B16F0 cells with drug-loaded LCP NPs substantially changed their morphology, as illustrated in Figure 6A. The untreated cells showed the natural spindle-like shape, which was transformed upon the treatment of drugs either in the free form or the LCP form. Furthermore, the cellular extensions were disrupted. Disruption of tubular extensions of tumor cells limits their access to nutrients (Siemann, 2011). Thus, cellular extension disruption not only inhibits tumor growth but is also vital for tumor cell dissemination and metastasis (Ross and Hunger, 2017). Similar morphological changes in MCF7 and MDA-MB-231

cells as a result of albendazole treatment is reported (Racoviceanu et al., 2020).

Morphological transformation and extension deformation by BMZ family drugs arise from their inhibition of tubulin polymerization (Kamal et al., 2012). This inhibition has been reported to alter microtubule organization of Chinese hamster cells after exposure to TBZ (Pisano et al., 2000), inducing abnormal spindle formation and enhanced tubulin depolymerization in non-small cell lung cancer cells treated with MBZ (Sasaki et al., 2002), and disruption of mitotic bundles in 1A9 ovarian cancer cells exposed to ABZ (Chu et al., 2009). Oxidative stress caused by BMZ drug treatment can also cause morphological changes and consequently motility alteration (Alexandrova et al., 2006).

Again, no obvious morphological changes such as spindle deformation or disruption of mitotic bundle was observed in HEK293T cells upon the similar treatment with BMZ family

(Figure 6B), which may be attributed to less susceptibility to ROS (Figure 5C) (Katoh et al., 2006).

As cells with more rounded shape are supposed to have less capability of dissemination because of the microtubule destabilization (Young et al., 1985), less migratory activity of BMZ drug-treated cells was observed, as shown in Figure 7A. All free BMZ family drugs inhibited cell migration to some degree at the dose of 2.5 µg/ml. Interestingly, their LCP forms were more effective in inhibition of cell migration by 15–30% in terms of the cell number (Figure 7B) and 20–40% in terms of the relative migration (Figure 7C), due to the enhanced solubility and cellular uptake in the LCP form. This inhibition results are comparable with previous studies about cell migration inhibition by BMZ family drugs. For instance, 24 h treatment of PE/CA-PJ15 cells (human oral squamous carcinoma) with 5 µM (~1.5 µg/ml) of FBZ and MBZ reduced cell migration very significantly (Kralova et al., 2018). Treatment with 0.6 µM (0.16 µg/ml) of ABZ halved migration activity of SW1990 and PANC-1 pancreatic cancer cells after 24 h treatment (Chen et al., 2020).

Since tumor cell migration is not only a prerequisite for tumor dissemination but also a contributor to tumor metastasis (Entschladen et al., 2004), inhibition of cell migration is vital for a comprehensive cancer treatment. Thus, BMZ family drugs, especially loaded in LCP NPs, may be considered as a treatment beyond the primary tumor inhibition, without obvious side effects to healthy cells or organs. This is a sharp contrast to other conventional chemotherapeutics such as paclitaxel, doxorubicin and cisplatin that are associated with various toxicities to healthy organs such as neurotoxicity, cardiotoxicity, nephrotoxicity, hepatotoxicity and hematotoxicity (Cersosimo, 1993; Juaristi et al., 2001; Guastalla and Diéras, 2003).

CONCLUSION

LCP nanoparticles provide a versatile nanoplatform to load anti-worm BMZ family drugs and repurpose their applications for cancer treatment. Having superior cytotoxic effect on cancer cells but almost no toxicity to healthy cells, BMZ drugs were successfully loaded by LCPs and showed even more efficient

inhibition of cancer cell proliferation via enhanced solubility and cellular uptake. We further found that BMZ drug-loaded LCPs induced more later apoptosis through Bcl-2 reduction and ROS augmentation. Moreover, BMZ-LCP NPs were able to control tumor cell dissemination through induction of morphological changes and inhibition of cell migration. Overall, LCP-based nanoformulated BMZ drugs would be considered as promising nanomedicines not only to treat primary tumors but also to potentially control tumor dissemination and metastasis with minimum side effects.

DATA AVAILABILITY STATEMENT

The original contributions presented in the study are included in the article/Supplementary Material, further inquiries can be directed to the corresponding author.

AUTHOR CONTRIBUTIONS

FM: Experimental WG: Co-supervision Associate CS: Co-supervision ZX: Supervision.

ACKNOWLEDGMENTS

The authors acknowledge financial supports from Australian Research Council (ARC) Discovery Projects (DP190103486). The authors also appreciate facilities and the technical assistance of the Australian Microscopy and Microanalysis Research Facility at the Center for Microscopy and Microanalysis (CMM), Australian National Fabrication Facility (Qld Node) and Center of Advance Imaging, The University of Queensland.

SUPPLEMENTARY MATERIAL

The Supplementary Material for this article can be found online at: <https://www.frontiersin.org/articles/10.3389/fnano.2021.693837/full#supplementary-material>

REFERENCES

- Alexandrova, A. Y., Kopnin, P. B., Vasiliev, J. M., and Kopnin, B. P. (2006). ROS Up-Regulation Mediates Ras-Induced Changes of Cell Morphology and Motility. *Exp. Cel. Res.* 312, 2066–2073. doi:10.1016/j.yexcr.2006.03.004
- Blanco, E., Shen, H., and Ferrari, M. (2015). Principles of Nanoparticle Design for Overcoming Biological Barriers to Drug Delivery. *Nat. Biotechnol.* 33, 941–951. doi:10.1038/nbt.3330
- Campbell, K. J., and Tait, S. W. G. (2018). Targeting BCL-2 Regulated Apoptosis in Cancer. *Open Biol.* 8, 180002. doi:10.1098/rsob.180002
- Carvalho, K. P., and Gadelha, A. P. R. (2007). Effects of Three Benzimidazoles on Growth, General Morphology and Ultrastructure of *Tritrichomonas Foetus*. *FEMS Microbiol. Lett.* 275, 292–300. doi:10.1111/j.1574-6968.2007.00897.x
- Castro, L. S. E. P. W., Kwiecinski, M. R., Ourique, F., Parisotto, E. B., Grinevicius, V. M. A. S., Correia, J. F. G., et al. (2016). Albendazole as a Promising Molecule for Tumor Control. *Redox. Biol.* 10, 90–99. doi:10.1016/j.redox.2016.09.013
- Cersosimo, R. J. (1993). Hepatotoxicity Associated with Cisplatin Chemotherapy. *Ann. Pharmacother.* 27, 438–441. doi:10.1177/106002809302700408
- Cha, H. J., Byrom, M., Mead, P. E., Ellington, A. D., Wallingford, J. B., and Marcotte, E. M. (2012). Evolutionarily Repurposed Networks Reveal the Well-Known Antifungal Drug Thiabendazole to Be a Novel Vascular Disrupting Agent. *Plos Biol.* 10, e1001379. doi:10.1371/journal.pbio.1001379
- Chen, X., Yao, X., Wang, C., Chen, L., and Chen, X. (2015). Hyperbranched PEG-Based Supramolecular Nanoparticles for Acid-Responsive Targeted Drug Delivery. *Biomater. Sci.* 3, 870–878. doi:10.1039/c5bm00061k
- Chen, H., Weng, Z., and Xu, C. (2020). Albendazole Suppresses Cell Proliferation and Migration and Induces Apoptosis in Human Pancreatic Cancer Cells. *Anticancer Drugs* 31, 431–439. doi:10.1097/CAD.0000000000000914
- Chu, S. W., Badar, S., Morris, D. L., and Pourgholami, M. H. (2009). Potent Inhibition of Tubulin Polymerisation and Proliferation of Paclitaxel-Resistant 1A9PTX22 Human Ovarian Cancer Cells by Albendazole. *Anticancer Res.* 29, 3791–3796. Available at: <http://www.ncbi.nlm.nih.gov/pubmed/19846910> (Accessed October 14, 2016)

- Daniel-Mwambete, K., Torrado, S., Cuesta-Bandera, C., Ponce-Gordo, F., and Torrado, J. J. (2004). The Effect of Solubilization on the Oral Bioavailability of Three Benzimidazole Carbamate Drugs. *Int. J. Pharm.* 272, 29–36. doi:10.1016/j.jipharm.2003.11.030
- Despommier, D. D., Gwadz, R. W., and Hotez, P. J. (2017). *Parasitic Diseases*, 6th Edn, New York: Springer
- Dogra, N., and Mukhopadhyay, T. (2012). Impairment of the Ubiquitin-Proteasome Pathway by Methyl N-(6-Phenylsulfanyl-1H-benzimidazol-2-yl) carbamate Leads to a Potent Cytotoxic Effect in Tumor Cells. *J. Biol. Chem.* 287, 30625–30640. doi:10.1074/jbc.M111.324228
- Dorosti, Z., Yousefi, M., Sharafi, S. M., and Darani, H. Y. (2014). Mutual Action of Anticancer and Antiparasitic Drugs: Are There Any Shared Targets? *Future Oncol.* 10, 2529–2539. doi:10.2217/fo.14.65
- Doudican, N., Rodriguez, A., Osman, I., and Orlow, S. J. (2008). Mebendazole Induces Apoptosis via Bcl-2 Inactivation in Chemoresistant Melanoma Cells. *Mol. Cancer Res.* 6, 1308–1315. doi:10.1158/1541-7786.MCR-07-2159
- Duan, Q., Liu, Y., and Rockwell, S. (2013). Fenbendazole as a Potential Anticancer Drug. *Anticancer Res.* 33, 355–362. Available at: <http://www.ncbi.nlm.nih.gov/pubmed/23393324> (Accessed April 3, 2020)
- Entschladen, F., Drell, T. L., Lang, K., Joseph, J., and Zaenker, K. S. (2004). Tumour-cell Migration, Invasion, and Metastasis: Navigation by Neurotransmitters. *Lancet Oncol.* 5, 254–258. doi:10.1016/S1470-2045(04)01431-7
- Guastalla, J. P., and Diéras, V. (2003). The Taxanes: Toxicity and Quality of Life Considerations in Advanced Ovarian Cancer. *Br. J. Cancer* 89 Suppl 3, S16–S22. doi:10.1038/sj.bjc.6601496
- Hasanpourghadi, M., Karthikeyan, C., Pandurangan, A. K., Looi, C. Y., Trivedi, P., Kobayashi, K., et al. (2016). Targeting of Tubulin Polymerization and Induction of Mitotic Blockage by Methyl 2-(5-Fluoro-2-Hydroxyphenyl)-1H-Benzo[d]imidazole-5-Carboxylate (MBIC) in Human Cervical Cancer HeLa Cell. *J. Exp. Clin. Cancer Res.* 35, 58. doi:10.1186/s13046-016-0332-0
- Hildeman, D. A., Mitchell, T., Aronow, B., Wojciechowski, S., Kappler, J., and Marrack, P. (2003). Control of Bcl-2 Expression by Reactive Oxygen Species. *Proc. Natl. Acad. Sci.* 100, 15035–15040. doi:10.1073/pnas.1936213100
- Juaristi, J. A., Aguirre, M. V., Carmuega, R. J., Romero-Benítez, M., Alvarez, M. A., and Brandan, N. C. (2001). Hematotoxicity Induced by Paclitaxel: *In Vitro* and *In Vivo* Assays during normal Murine Hematopoietic Recovery. *Methods Find Exp. Clin. Pharmacol.* 23, 161–167. doi:10.1358/mf.2001.23.4.634639
- Kamal, A., Reddy, M., Shaik, T. B., Rajender, R., Srikanth, Y., Reddy, V. S., et al. (2012). Synthesis of Terphenyl Benzimidazoles as Tubulin Polymerization Inhibitors. *Eur. J. Med. Chem.* 50, 9–17. doi:10.1016/j.ejmech.2012.01.004
- Kang, B.-S., Lee, S.-E., Ng, C., Kim, J.-K., and Park, J.-S. (2015). Exploring the Preparation of Albendazole-Loaded Chitosan-Tripolyphosphate Nanoparticles. *Materials* 8, 486–498. doi:10.3390/ma8020486
- Katoh, H., Hiramoto, K., and Negishi, M. (2006). Activation of Rac1 by RhoG Regulates Cell Migration. *J. Cel. Sci.* 119, 56–65. doi:10.1242/jcs.02720
- Kohane, D. S. (2007). Microparticles and Nanoparticles for Drug Delivery. *Biotechnol. Bioeng.* 96, 203–209. doi:10.1002/bit.21301
- Kralova, V., Hanušová, V., Caltová, K., Špaček, P., Hochmalová, M., Skálová, L., et al. (2018). Flubendazole and Mebendazole Impair Migration and Epithelial to Mesenchymal Transition in Oral Cell Lines. *Chem. Biol. Interact.* 293, 124–132. doi:10.1016/j.cbi.2018.07.026
- Kumar, R., Dalvi, S. V., and Siril, P. F. (2020). Nanoparticle-Based Drugs and Formulations: Current Status and Emerging Applications. *ACS Appl. Nano Mater.* 3, 4944–4961. doi:10.1021/acsnano.0c00606
- Liu, J., Yu, M., Zhou, C., and Zheng, J. (2013). Renal Clearable Inorganic Nanoparticles: A New Frontier of Bionanotechnology. *Mater. Today* 16, 477–486. doi:10.1016/j.matod.2013.11.003
- Melian, M. E., Paredes, A., Munguía, B., Colobbio, M., Ramos, J. C., Teixeira, R., et al. (2020). Nanocrystals of Novel Valerolactam-Fenbendazole Hybrid with Improved *In Vitro* Dissolution Performance. *AAPS PharmSciTech* 21, 1–15. doi:10.1208/s12249-020-01777-y
- Movahedi, F., Wu, Y., Gu, W., and Xu, Z. P. (2020). Nanostructuring a Widely Used Antiworm Drug into the Lipid-Coated Calcium Phosphate Matrix for Enhanced Skin Tumor Treatment. *ACS Appl. Bio Mater.* 3, 4230–4238. doi:10.1021/acsbm.0c00313
- Mukhopadhyay, T., Sasaki, J., Ramesh, R., and Roth, J. A. (2002). Mebendazole Elicits a Potent Antitumor Effect on Human Cancer Cell Lines Both *In Vitro* and *In Vivo*. *Clin. Cancer Res.* 8, 2963–2969.
- Noorani, L., Stenzel, M., Liang, R., Pourgholami, M. H., and Morris, D. L. (2015). Albumin Nanoparticles Increase the Anticancer Efficacy of Albendazole in Ovarian Cancer Xenograft Model. *J. Nanobiotechnol* 13, 25. doi:10.1186/s12951-015-0082-8
- Patel, K., Doudican, N. A., Schiff, P. B., and Orlow, S. J. (2011). Albendazole Sensitizes Cancer Cells to Ionizing Radiation. *Radiat. Oncol.* 6, 160. doi:10.1186/1748-717X-6-160
- Perillo, B., Di Donato, M., Pezone, A., Di Zazzo, E., Giovannelli, P., Galasso, G., et al. (2020). ROS in Cancer Therapy: The Bright Side of the Moon. *Exp. Mol. Med.* 52, 192–203. doi:10.1038/s12276-020-0384-2
- Pfeffer, C. M., and Singh, A. T. K. (2018). Apoptosis: A Target for Anticancer Therapy. *Int. J. Mol. Sci.* 19, 448. doi:10.3390/ijms19020448
- Pisano, C., Battistoni, A., Antocchia, A., Degrassi, F., and Tanzarella, C. (2000). Changes in Microtubule Organization after Exposure to a Benzimidazole Derivative in Chinese Hamster Cells. *Mutagenesis* 15, 507–515. doi:10.1093/mutage/15.6.507
- Pushpakom, S., Iorio, F., Eyers, P. A., Escott, K. J., Hopper, S., Wells, A., et al. (2018). Drug Repurposing: Progress, Challenges and Recommendations. *Nat. Rev. Drug Discov.* 18, 41–58. doi:10.1038/nrd.2018.168
- Racoviceanu, R., Trandafirescu, C., Voicu, M., Ghiulai, R., Borcan, F., Dehelean, C., et al. (2020). Solid Polymeric Nanoparticles of Albendazole: Synthesis, Physico-Chemical Characterization and Biological Activity. *Molecules* 25, 5130. doi:10.3390/molecules25215130
- Ross, C., and Hunger, K. (2017). “Metastatic Signatures-The Tell-Tale Signs of Metastasis,” in *Encyclopedia Of Cancer*. Elsevier, 426–434. doi:10.1016/B978-0-12-801238-3.65027-4
- Ryu, J.-H., Diakur, J., Kelly, S., Russell, J., and Wiebe, L. (2013). A Water-Soluble Fenbendazole (FBZ) Formulation for Treating Pinworm Infections in Laboratory Animals. *Ddl* 3, 159–164. doi:10.2174/2210303111303030001
- Sasaki, J., Ramesh, R., Chada, S., Gomyo, Y., Roth, J. A., and Mukhopadhyay, T. (2002). The Anthelmintic Drug Mebendazole Induces Mitotic Arrest and Apoptosis by Depolymerizing Tubulin in Non-small Cell Lung Cancer Cells. *Mol. Cancer Ther.* 1201–9. Available at: <http://www.ncbi.nlm.nih.gov/pubmed/12479701> (Accessed May 3, 2016).
- Siemann, D. W. (2011). The Unique Characteristics of Tumor Vasculature and Preclinical Evidence for its Selective Disruption by Tumor-Vascular Disrupting Agents. *Cancer Treat. Rev.* 37, 63–74. doi:10.1016/j.ctrv.2010.05.001
- Stasiuk, S. J., MacNevin, G., Workentine, M. L., Gray, D., Redman, E., Bartley, D., et al. (2019). Similarities and Differences in the Biotransformation and Transcriptomic Responses of *Caenorhabditis elegans* and *Haemonchus contortus* to Five Different Benzimidazole Drugs. *Int. J. Parasitol. Drugs Drug Resist.* 11, 13–29. doi:10.1016/j.ijpddr.2019.09.001
- Swanepoel, E., Liebenberg, W., Devarakonda, B., and De Villiers, M. M. (2003). Developing a Discriminating Dissolution Test for Three Mebendazole Polymorphs Based on Solubility Differences. *Pharmazie* 58 (2), 117–121. Available at: https://www.researchgate.net/publication/10852995_Developing_a_discriminating_dissolution_test_for_three_mebendazole_polymorphs_based_on_solubility_differences (Accessed May 17, 2021)
- Tang, J., Li, L., Howard, C. B., Mahler, S. M., Huang, L., and Xu, Z. P. (2015). Preparation of Optimized Lipid-Coated Calcium Phosphate Nanoparticles for Enhanced *In Vitro* Gene Delivery to Breast Cancer Cells. *J. Mater. Chem. B* 3, 6805–6812. doi:10.1039/C5TB00912J
- Thiabendazole - DrugBank. Available at: <https://www.drugbank.ca/drugs/DB00730> (Accessed May 3, 2020).
- Thorat, A. A., and Dalvi, S. V. (2012). Liquid Antisolvent Precipitation and Stabilization of Nanoparticles of Poorly Water Soluble Drugs in Aqueous Suspensions: Recent Developments and Future Perspective. *Chem. Eng. J.* 181–182, 1–34. doi:10.1016/j.cej.2011.12.044

- Wu, Y., Gu, W., Tang, J., and Xu, Z. P. (2017). Devising New Lipid-Coated Calcium Phosphate/carbonate Hybrid Nanoparticles for Controlled Release in Endosomes for Efficient Gene Delivery. *J. Mater. Chem. B* 5, 7194–7203. doi:10.1039/C7TB01635B
- Young, M. R., Newby, M., and Meunier, J. (1985). Relationships between Morphology, Dissemination, Migration, and Prostaglandin E2 Secretion by Cloned Variants of Lewis Lung Carcinoma. *Cancer Res.* 45, 3918–3923.
- Zhang, L., Bochkur Dratver, M., Yazal, T., Dong, K., Nguyen, A., Yu, G., et al. (2019). Mebendazole Potentiates Radiation Therapy in Triple-Negative Breast Cancer. *Int. J. Radiat. Oncology*Biophysics* 103, 195–207. doi:10.1016/j.ijrobp.2018.08.046

Conflict of Interest: The authors declare that the research was conducted in the absence of any commercial or financial relationships that could be construed as a potential conflict of interest.

Copyright © 2021 Movahedi, Gu, Soares and Xu. This is an open-access article distributed under the terms of the Creative Commons Attribution License (CC BY). The use, distribution or reproduction in other forums is permitted, provided the original author(s) and the copyright owner(s) are credited and that the original publication in this journal is cited, in accordance with accepted academic practice. No use, distribution or reproduction is permitted which does not comply with these terms.